Progress In Electromagnetics Research Letters, Vol. 85, 117–123, 2019

A Terahertz Quarter Wave Plate Based on Staggered Split Ring Resonators

Wu Pan, Xinyu Ren*, and Qi Chen

Abstract—In this paper, we propose a transmissive quarter wave plate (QWP) which can provide linear-to-circular polarization conversion in terahertz (THz). The structure is composed of one dielectric layer with staggered split ring resonators (SSRRs) on both sides. The simulation results show that the proposed structure can offer a nearly pure left circularly polarized wave with 3 dB axial ratio bandwidth of 0.337 THz; meanwhile, the bandwidth of polarization conversion efficiency beyond 80% reaches 0.170 THz. Additionally, the distributions of surface currents and electric field are discussed to explain the physical mechanism of the proposed structure. The linear-to-circular polarization conversion can be attributed to the inductance effect and capacitance effect between SSRRs. Finally, we validate the performance of the proposed THz-QWP. Such a device could potentially be used in THz communications, THz imaging, and THz sensing.

1. INTRODUCTION

The development of metamaterials has brought a series of progress in THz devices, such as THz antennas, THz sensors, and THz modulators. Compared with traditional materials, metamaterials can achieve arbitrary values of permittivity and permeability, which open up a new way towards efficient manipulation of electromagnetic (EM) wave for their intriguing properties. Among all the properties of EM wave, polarization plays an important role for its multiple applications, such as communication system and sensing system. Because of the exotic properties of metamaterials, the high performance polarization controller based on metamaterial is urgently needed, especially for the THz band.

Great efforts have been made to improve the performance of THz-QWP. Common THz-QWP approximately includes three types: split ring resonators (SRRs) [1], cross-shaped resonators [2], and meander-line [3]. Based on the ring-cross resonators, Zhang et al. [4] proposed a QWP which can convert $\pm 45^\circ$ polarized incident wave into the left (right) circularly polarized wave between 10.8 and 12.8 GHz. The resonator consists of a ring and a centrally placed cross, which contribute to the electric resonance and magnetic resonance. Cheng and Cheng [5] investigated a chiral metamaterial based on asymmetry bilayer conjugated SRRs by applying the traditional SRRs. When normal incident light is propagating along the $-z$ axis direction through the proposed structure, the y-polarized waves will be converted into the left and right circularly polarized waves at 1.14 THz and 1.34 THz, respectively. To achieve the broadband circular polarizer, Mangi et al. [6] introduced an SRRs array pattern on the top and bottom interfaces of the substrate. The incident co-polarization and cross-polarization waves achieved high transmission behaviors and were successfully converted into circular polarization wave in the range of 13.94–15.70 GHz.

In this paper, a transmissive QWP based on SSRRs is proposed and investigated. The staggered arrangement is adopted to enhance the coupling between adjacent SRRs. The proposed QWP

Received 15 March 2019, Accepted 20 June 2019, Scheduled 27 June 2019

* Corresponding author: Xinyu Ren (rxyindex@163.com).

The authors are with the College of Photoelectric Engineering, Chongqing University of Posts and Telecommunications, Chongqing 400065, China.

can convert the incident linear polarized wave into left circularly polarized wave in the range of $0.550 \sim 0.887$ THz. The physical mechanism of our structure is to make an array of structures which appear inductive to one polarization and capacitive to orthogonal polarization [7]. Finally, the sample of our design is fabricated to validate the simulation.

2. DESIGN AND SIMULATION

2.1. Structure Design

In Fig. 1(a), the three-dimensional structure of proposed THz-QWP is schematically presented, which is composed of two metallic layers separated by a dielectric film. Besides, the metallic layers on either side of the dielectric layer have same pattern as shown in Fig. 1(a). The periodicity of the unit cell is 140 µm. The thicknesses of the dielectric layer and metal layer are 50 µm and 0.2 µm, respectively. The dielectric layer is selected as quartz with a relative permittivity of 3.5 and dielectric loss tangent of 0.0027. The metallic layer is modeled as a gold film with an electric conductivity $\sigma = 4.561 \times 10^7$ S/m. The top view of the metallic layer is shown in Fig. 1(b). The rest of geometric parameters are as follows: $L_1 = 52$ µm, $L_2 = 46$ µm, $L_3 = 46$ µm, $L_4 = 66$ µm.

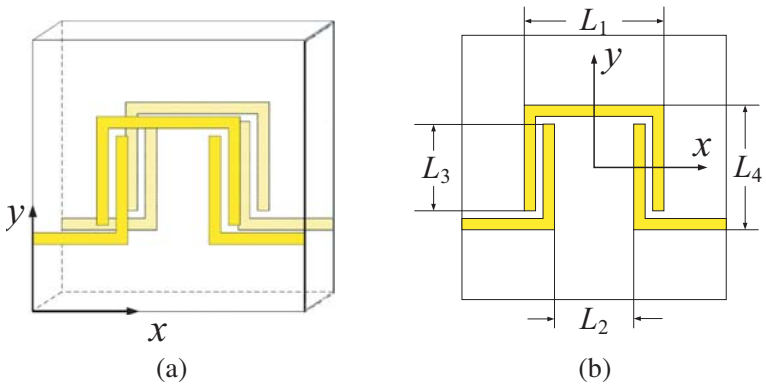

Figure 1. Schematic of the unit cell of proposed THz-QWP. (a) The three-dimensional graphic; (b) The top view.

The numerical simulation is carried out to investigate the polarization conversion behaviors of the QWP by CST MICROWAVE STUDIO 2017 with unit cell boundary conditions. The linearly polarized wave at 45° is applied to excite the metamaterial along the $-z$ direction. Since one of the group elements of our structure is σ_z, the transmission behaviors are the same regardless of the direction of the incident wave along the $+z$ or $-z$ direction.

To evaluate the polarization state of output waves, the Stokes parameters are calculated with the following equations: $S = |t_{ox}|^2 + |t_{oy}|^2$, $S_1 = |t_{ox}|^2|t_{oy}|^2$, $S_2 = 2 \cdot |t_{ox}| \cdot |t_{oy}| \cdot \cos(\Delta\varphi)$, $S_3 = 2 \cdot |t_{ox}| \cdot |t_{oy}| \cdot \sin(\Delta\varphi)$ where $|t_{ox}|$ and $|t_{oy}|$ are the magnitudes of the transmission coefficients along x- and y-axes, and $\Delta\varphi$ is the phase delay between them. As for the output waves, S and S_1 are the sum and difference of the intensities of the two orthogonal components; S_2 represents the excess intensity of the $+45°$ linear polarized part over the $-45°$ linear polarized part; and S_3 is the excess intensity in the spectral density of the right circularly polarized component over the left circularly polarized one [8]. Based on the Stokes parameters, the polarization azimuth angle can be defined as $\alpha = 0.5 \times \arctan(S_2/S_1)$, and the ellipticity angle can be defined as $\beta = 0.5 \times \arctan(S_3/S)$. The ellipticity $\chi = S_3/S$. The polarization azimuth angle α describes the direction of the principal axis of ellipse, and the ellipticity χ describes the shape of polarization ellipse. The axis ratio (AR) and polarization conversion efficiency (PCE) can be calculated as: $\mathrm{AR} = 10\lg(\tan\beta)$, $\mathrm{PCE} = [|t_{ox}|^2 + |t_{oy}|^2]/[|t_{ix}|^2 + |t_{iy}|^2]$, where subscripts $i(o)x$ and $i(o)y$ correspond to the input (output) THz waves along x-axis and y-axis, respectively. When AR is smaller than 3 dB, the device could be as functional as a QWP [9].

2.2. Simulation Results

To confirm the validity of polarization conversion, transmission responses of our structure under x- and y-polarized waves are investigated, and results are displayed in Fig. 2. As the spectra presented in Fig. 2(a), the transmission coefficients are within the range of 0.75 to 1.00 around $0.60 \sim 0.85$ THz along x- and y-axes. As shown in Fig. 2(b), a continuing near $\pi/2 \pm \pi$ phase difference between the two orthogonal polarizations is achieved at the same frequency range. According to the basic physical principle, the circularly polarized waves can be equivalent to two orthogonal polarizations with equal magnitude and 90° difference in phase. Thus, the output waves can be seen as circularly polarized waves.

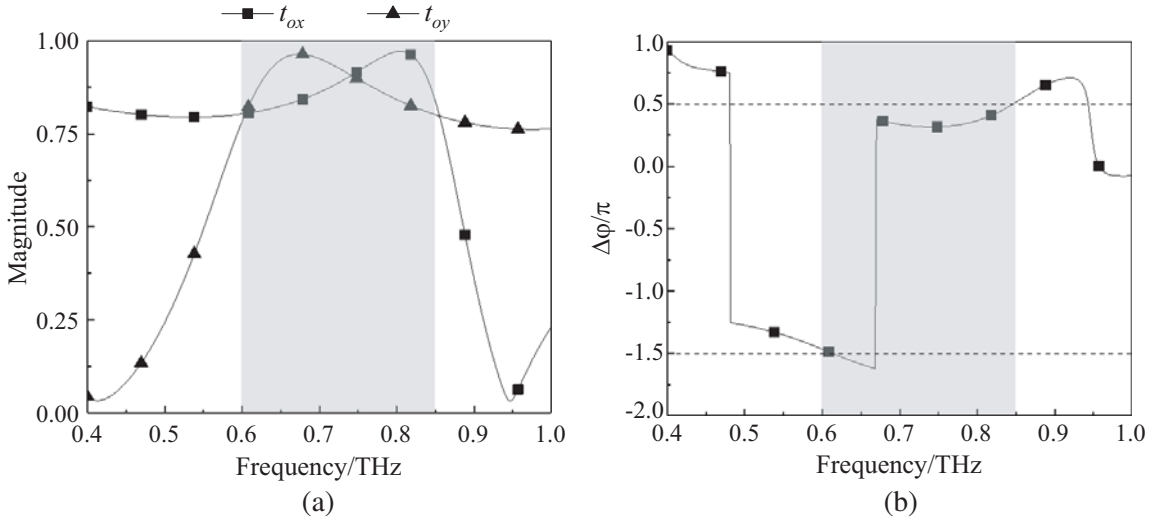

Figure 2. Simulated transmission coefficients of proposed THz-QWP, along x- and y-axes. (a) Magnitude; (b) Phase difference.

To evaluate the performance of designed QWP, the AR and PCE are introduced. As shown in Fig. 3, since the AR between 0.550 and 0.887 THz is less than 3 dB, the proposed structure can be functional for a THz-QWP according to [9]. The efficiency of polarization conversion is also presented in Fig. 3, which is more than 80% in the range of 0.650–0.820 THz. A metamaterial-based QWP with

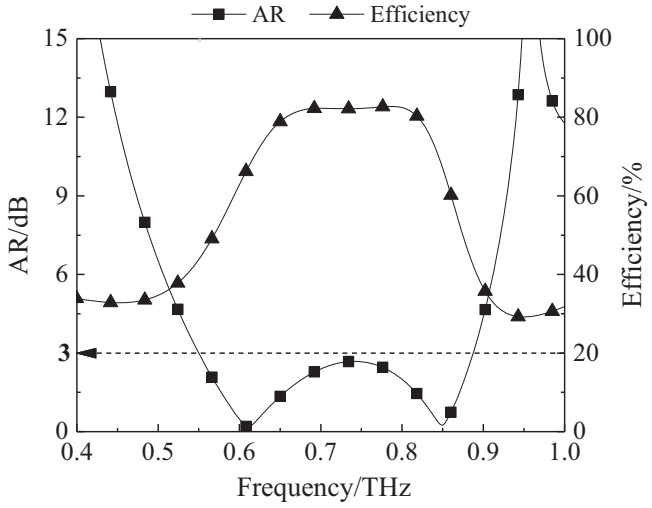

Figure 3. The simulated AR and efficiency of proposed THz-QWP.

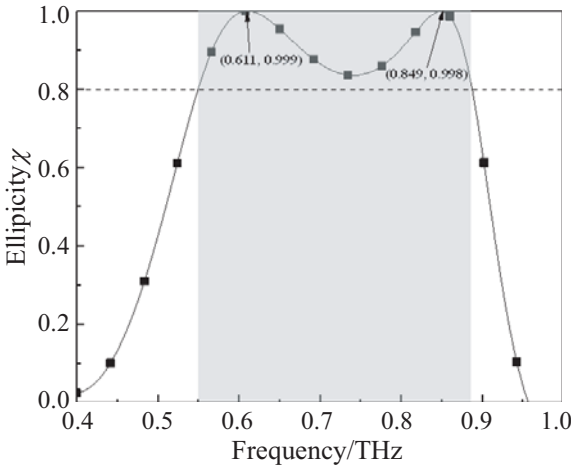

Figure 4. The simulated ellipticities of proposed THz-QQWP.

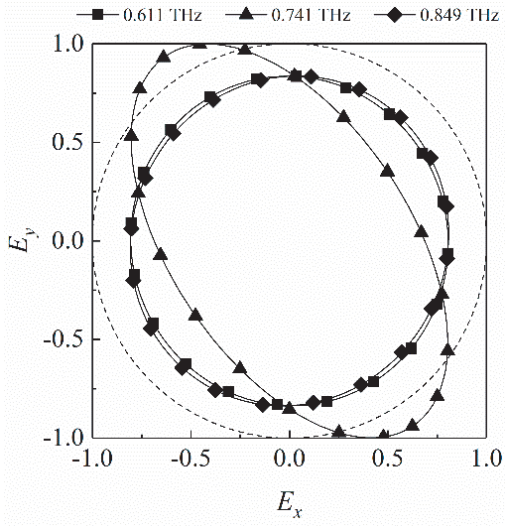

Figure 5. The simulated normalized polarization ellipses of transmitted wave. Circle of dotted line is an ideal normalized polarization ellipse.

high efficiency is achieved.

The simulated ellipticities are shown in Fig. 4. Two maximum values of ellipticities are achieved at 0.611 THz and 0.849 THz, and a minimal value at 0.741 THz. The near unity ellipticities reveal that the transmitted wave is left circularly polarized wave. The visual performance of transmitted wave is given in Fig. 5. It can be seen that the shapes of simulated normalized polarization ellipses approach an ideal circle, which indicates that the proposed QWP successfully converts the incident linearly polarized wave into left circularly polarized wave.

2.3. Analysis Based on Surface Currents and Electric Field

The distributions of surface currents on the metal layers are given in Fig. 6. The black arrows indicate the direction of currents. According to the directions of those arrows, one can know what kind of EM

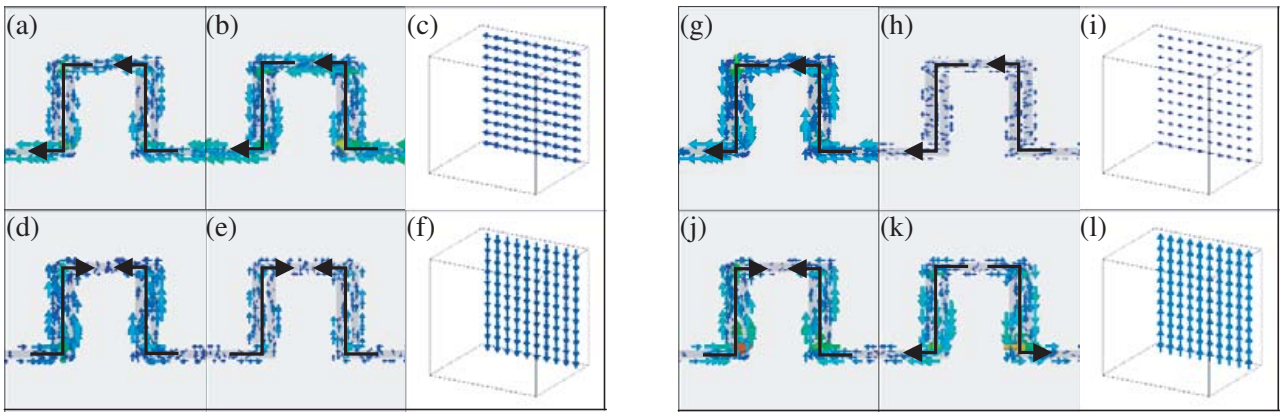

Figure 6. At 0.611 THz, the distributions surface currents of the front and back metal layers for incident (a), (b) x, and (d), (e) y-polarized waves. At 0.611 THz, the electric field directed along the (c) x- and (f) y-axes for output wave. At 0.849 THz, the distributions surface currents of the front and back metal layers for incident (g), (h) x, and (j), (k) y-polarized waves. At 0.849 THz, the electric field directed along the (i) x- and (l) y-axes for output wave.

coupling is happening. For the case of x-polarized incident wave, the unit cell behaves as an inductance. The surface currents flow along $-x$ direction, which is induced by the incident wave polarized along the opposite x axis, as shown in Figs. 6(a), (b), (g), (h). As for the incident y-polarized wave, the unit cell behaves as a capacitance, as shown in Figs. 6(d), (e), (j), (k).

According to polarization decomposition theory, the output wave can be equalized into two orthogonal linear polarized waves, as shown in Figs. 6(c), (f), (i), (l). The output wave is circularly polarized wave which consists of two orthogonal linearly polarized waves with $\Delta\varphi \approx \pi/2 \pm \pi$, as shown in Figs. 6(c), (f) and Figs. 6(i), (l). It is worth noting that the surface currents and electric field in Fig. 6(k) are in the reverse direction relative to Figs. 6(b), (e), (h). The phase reverse is a symbol of equivalent circuit of metamaterials. The equivalent circuit of metamaterials changes in different frequency bands.

3. FABRICATION AND MEASUREMENT

To experimentally prove the previous simulation results, the designed THz-QWP is fabricated, and its transmission coefficients for incident linear polarized waves are measured with terahertz time domain spectroscopy (THz-TDS, Z3). The sample is excited by the x and y linearly polarized waves, successively. Furthermore, the sample should be hold gently in the process of experiment for fear of crush. The microscope image of 4×4 unit cells is shown in Fig. 7. The magnitudes of measured transmission coefficients for two orthogonal linearly polarized waves are shown in Fig. 8(a), and the phase difference is shown in Fig. 8(b). The measured results shown in Fig. 8 have a discrepancy compared to simulated data in Fig. 2 that can be attributed on the misalignment between front metal layer and back metal layer. Furthermore, the angular misalignment between our sample and the direction of probe waves should be blamed.

Table 1 is provided to compare the performance (3 dB AR bandwidth and efficiency) of our design with the earlier reported QWP. The AR of our device between 0.550 and 0.887 THz is less than 3 dB,

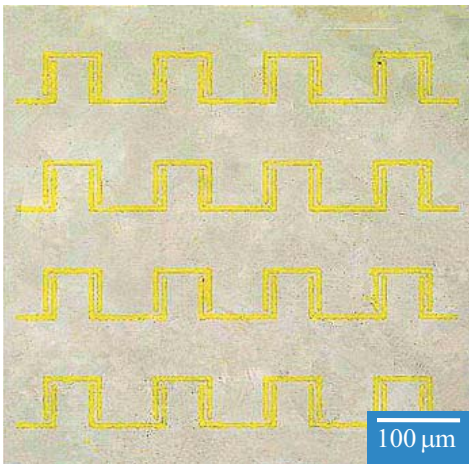

Figure 7. Microscope image of the fabricated sample.

Table 1. Comparison with some other reported THz-QWP.

THz-QWP	Frequency Range (AR $<$ 3 dB)	PCE
Wang et al. [10]	0.75 $\sim$ 0.95 THz	$\sim$ 40%
Zhu et al. [11]	0.60 $\sim$ 0.85 THz	—
Han et al. [12]	0.90 $\sim$ 1.10 THz	60 $\sim$ 80%
Zang et al. [13]	0.78 $\sim$ 1.08 THz	70 $\sim$ 80%
Proposed QWP	0.65 $\sim$ 0.82 THz	$\sim$ 80%

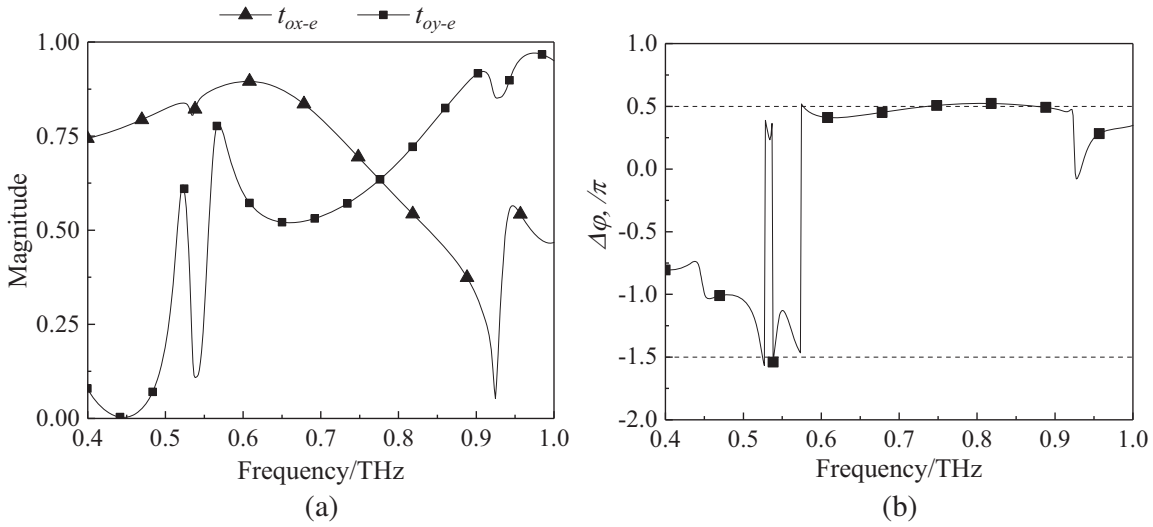

Figure 8. Measured transmission coefficients of proposed THz-QWP for x- and y-polarized waves. (a) Magnitude; (b) Phase difference.

and the efficiency of polarization conversion is more than 80% in the range of 0.650–0.820 THz, as shown in Fig. 3. It can be seen that our design exhibits great advantages compared with the earlier reported designs in Table 1. It should be noted that the first three structures and proposed QWP are transmission type, and the fourth is reflection type which usually has a better performance than transmission type.

4. CONCLUSION

In this paper, a THz-QWP based on SSRRs has been experimentally and numerically demonstrated. Our device can convert 45° linearly polarized wave into left circularly polarized wave from 0.550 to 0.887 THz; meanwhile, the bandwidth of PCE above 80% reaches 0.170 THz. The polarization conversion can be attributed to the inductance and capacitance, which are induced by incident linearly polarized waves. Compared with previous research, the proposed device provides a better performance for linear to circular polarization conversion. Our device will have an extensive range of applications in THz communications, THz imaging, and THz sensing.

ACKNOWLEDGMENT

This work was supported by New Direction Cultivation Project of Chongqing University of Posts and Telecommunications (A2014-116).

REFERENCES

1. Nouman, M. T., J. H. Hwang, M. Faiyaz, et al., "Vanadium dioxide based frequency tunable metasurface filters for realizing reconfigurable terahertz optical phase and polarization control," *Optics Express*, Vol. 26, No. 10, 12922–12929, 2018.
2. Wang, D., L. Zhang, Y. Gu, et al., "Switchable ultrathin quarter-wave plate in terahertz using active phase-change metasurface," *Scientific Reports*, Vol. 5, 15020, 2015.
3. Strikwerda, A. C., K. Fan, H. Tao, et al., "Comparison of birefringent electric split-ring resonator and meander-line structures as quarter-wave plates at terahertz frequencies," *Optics Express*, Vol. 17, No. 1, 136–149, 2009.

4. Zhang, Z., X. Cao, J. Gao, et al., "Polarization-dependent multi-functional metamaterial as polarization filter, transparent wall and circular polarizer using ring-cross resonator," *Radio Engineering*, Vol. 26, No. 3, 705–712, 2017.
5. Cheng, Z. and Y. Cheng, "A multi-functional polarization convertor based on chiral metamaterial for terahertz waves," *Optics Communications*, Vol. 435, 178–182, 2019.
6. Mangi, F. A., S. Xiao, Z. Yao, et al., "Double-layer broadband circular polarizer based on fission transmission of linear polarization for ku-band applications," *Microwave and Optical Technology Letters*, Vol. 59, No. 10, 2680–2685, 2017.
7. Young, L., L. Robinson, and C. Hacking, "Meander-line polarizer," *IEEE Transactions on Antennas and Propagation*, Vol. 21, No. 3, 376–378, 1973.
8. He, J., Z. Xie, S. Wang, et al., "Terahertz polarization modulator based on metasurface," *Journal of Optics*, Vol. 17, No. 10, 105107, 2015.
9. Akgol, O., O. Altintas, E. Unal, et al., "Linear to left- and right-hand circular polarization conversion by using a metasurface structure," *International Journal of Micro-wave and Wireless Technologies*, Vol. 10, No. 1, 133–138, 2018.
10. Wang, D., Y. Gu, Y. Gong, et al., "An ultrathin terahertz quarter-wave plate using planar babinet-inverted metasurface," *Optics Express*, Vol. 23, No. 9, 11114–11122, 2015.
11. Zhu, L., L. Dong, J. Guo, et al., "Polarization conversion based on mie-type Electromagnetically Induced Transparency (EIT) effect in all-dielectric metasurface," *Plasmonics*, Vol. 13, No. 6, 1971–1976, 2018.
12. Han, Z., S. Ohno, Y. Tokizane, et al., "Off-resonance and in-resonance metamaterial design for a high-transmission terahertz-wave quarter-wave plate," *Optics Letters*, Vol. 43, No. 12, 2977–2980, 2018.
13. Zang, X., S. Liu, H. Gong, et al., "Dual-band superposition induced broadband terahertz linear-to-circular polarization converter," *Journal of the Optical Society of America B*, Vol. 35, No. 4, 950–957, 2018.